2010

A Polymorphic Variant of AFAP-110 Enhances cSrc Activity12

David A. Clump
West Virginia University

Jing J. Yu
West Virginia University

YoungJin Cho
West Virginia University

Rui Gao
National Cancer Institute

John Jett
West Virginia University

See next page for additional authors

Translational Oncology
www.transonc.com

Volume 3 Number 4 August 2010 pp. 276–285 276

A Polymorphic Variant of AFAP-110 Enhances cSrc Activity[1,2]

David A. Clump*,[3], Jing Jie Yu[†], YoungJin Cho*,[4], Rui Gao[‡], John Jett[§], Henry Zot[¶], Jess M. Cunnick[#,4], Brandi Snyder[†], Anne C. Clump*, Melissa Dodrill*, Peter Gannett[§], James E. Coad, Robert Shurina[††], W. Douglas Figg[‡], Eddie Reed[‡‡] and Daniel C. Flynn*,[4]**

*The Mary Babb Randolph Cancer Center and the Department of Microbiology, Immunology and Cell Biology, West Virginia University, Morgantown, WV, USA; [†]The Mary Babb Randolph Cancer Center and the Department of Biochemistry, West Virginia University, Morgantown, WV, USA; [‡]Molecular Pharmacology Section, Medical Oncology Branch, Center for Cancer Research, National Cancer Institute, National Institutes of Health, Bethesda, MD, USA; [§]Department of Basic Pharmaceutical Sciences, West Virginia University, Morgantown, WV, USA; [¶]Department of Biology, University of West Georgia, Carrolton, GA, USA; [#]The Mary Babb Randolph Cancer Center and the Department of Pathology, West Virginia University, Morgantown, WV, USA; **Department of Pathology, West Virginia University, Morgantown, WV, USA; [††]Department of Biology, Wheeling Jesuit University, Wheeling, WV, USA; [‡‡]Division of Cancer Prevention and Control, National Center for Chronic Disease Prevention and Health Promotion, CoCHP, The Centers for Disease Control and Prevention, Atlanta, GA, USA

Abstract

Enhanced expression and activity of cSrc are associated with ovarian cancer progression. Generally, cSrc does not contain activating mutations; rather, its activity is increased in response to signals that affect a conformational change that releases its autoinhibition. In this report, we analyzed ovarian cancer tissues for the expression of a cSrc-activating protein, AFAP-110. AFAP-110 activates cSrc through a direct interaction that releases it from its autoinhibited conformation. Immunohistochemical analysis revealed a concomitant increase of AFAP-110 and cSrc in ovarian cancer tissues. An analysis of the AFAP-110 coding sequence revealed the presence of a nonsynonymous, single-nucleotide polymorphism that resulted in a change of Ser403 to Cys403. In cells that express enhanced levels of cSrc, AFAP-110^{403C} directed the activation of cSrc and the formation of podosomes independently of input signals, in contrast to wild-type AFAP-110. We therefore propose that, under conditions of cSrc overexpression, the polymorphic variant of AFAP-110 promotes cSrc activation. Further, these data indicate a mechanism by which an inherited genetic variation could influence ovarian cancer progression and could be used to predict the response to targeted therapy.

Translational Oncology (2010) 3, 276–285

Address all correspondence to: Daniel C. Flynn, PhD, The Commonwealth Medical College, 501 Madison Ave, Scranton, PA 18510. E-mail: dflynn@tcmedc.org
[1]This work was supported by grants from the National Institutes of Health (CA60731 and RR16440), the Pardee Foundation (D.C.F.), and the West Virginia University Medical Scientists Training Program (D.A.C.). The authors declare no conflict of interest.
[2]This article refers to supplementary materials, which are designated by Tables W1 and W2 and Figure W1 and are available online at www.transonc.com.
[3]Current address: University of Pittsburgh Medical Center, Radiation Oncology, 5230 Centre Ave, Pittsburgh, PA 15231.
[4]Current address: The Commonwealth Medical College, 501 Madison Ave, Scranton, PA 18510.
Received 7 January 2010; Revised 18 March 2010; Accepted 31 March 2010

DOI 10.1593/tlo.10106

Introduction

Ovarian cancer, the most lethal gynecologic malignancy, is characterized by tumor disruption of the ovarian capsule and dissemination and seeding of the pelvic and abdominal cavities [1]. A combination of unreliable screening techniques, unspecific symptoms, and chemotherapy resistance results in 15,000 mortalities per year in the United States [2]. *BRCA1* and *BRCA2* are relevant for the disease, and mutations of these genes are found in approximately 15% of ovarian cancer cases [3,4]. However, most cases consist of inconspicuous associations between inherited susceptibility and the environment. These associations may be explained by haplotype mapping studies, which predict that single-nucleotide polymorphisms (SNPs) are not inherited independently, but instead associate with one another, as well as with environmental stimuli, producing the disease [5]. Whereas SNPs that influence drug metabolism and cancer-related symptoms are described [6], little is known about genetic variants that modulate tumorigenesis. Identification of these genes may enhance our understanding of the progression of neoplasms such as ovarian cancer. In addition, these polymorphisms may serve as biomarkers that predict susceptibility to cancer or response to therapy.

One protein contributing to ovarian cancer progression is cSrc. This tyrosine kinase is overexpressed and activated in ovarian cancer cell lines and ovarian tumors [7]. cSrc promotes motility and invasion, alteration of adhesion, and epithelial-mesenchymal transition [8,9]. In addition, cSrc contributes to chemotherapy resistance because inhibiting cSrc restores sensitivity to paclitaxel [10,11]. cSrc activation does not correlate with intrinsic mutations or SNPs; rather, signals from growth factors in the tumor microenvironment or intracellular activators of cSrc direct cSrc activation. A few cSrc activators have genetic variations that potentially modulate cSrc activity [10,11], and these may eventually serve as biomarkers useful for identifying the tumors most likely to respond to cSrc inhibition.

One cSrc activator, the actin-filament associated protein of 110 kDa (AFAP-110) is encoded by a polymorphic gene. The National Center for Biotechnology Information dsSNP database identifies a nonsynonymous C1210G coding substitution in exon 9 that predicts a serine-to-cysteine change at amino acid 403 (AFAP-110^{403C}) (http://www.ncbi.nlm.nih.gov/SNP/snp_ref.cgi?locusId=60312). AFAP-110, through its intrinsic multimerization and a carboxy-terminal actin-binding domain, promotes actin filament cross-linking [12,13]. In addition, AFAP-110 relays signals from protein kinase C α (PKCα) that activates cSrc [14,15]. These functions are autoinhibited by an intermolecular interaction between the carboxy-terminal leucine zipper motif and an amino-terminal pleckstrin homology domain (PH1) [13,15]. On experimental deletion of the leucine zipper domain (AFAP-$110^{\Delta Lzip}$) or on PKCα activation, AFAP-110 is uninhibited and facilitates cSrc activation [13,15]. This correlates with trafficking of activated cSrc to the cell membrane and the formation of the actin-rich invasive structures—podosomes [14,16].

To determine whether AFAP-110 is positioned to activate cSrc in ovarian cancer, we performed immunohistochemical analysis on ovarian cancer tissues. In doing so, we demonstrated that AFAP-110 exhibited a concomitant increase in expression with cSrc. Using polymerase chain reaction (PCR) analysis, we discovered that a polymorphism of AFAP-110 was expressed in one-fourth of the population. This polymorphic variant, AFAP-110^{403C}, activated cSrc and triggered the formation of podosomes, suggesting that this variant of AFAP-110 may contribute to the progression of ovarian cancer.

Materials and Methods

Reagents

The rabbit anti–human cortactin polyclonal antibody was purchased from Abcam (Cambridge, MA). The AFAP-110 antibody F1 was previously characterized [17]. The mouse anti–avian Src monoclonal antibody (clone EC10) was obtained from Upstate Biotechnology (Lake Placid, NY). The rabbit anti–human cSrc monoclonal antibody (clone EG107) was from Novus Biologicals (Littleton, CO). The rabbit anti–phospho-Src (Tyr416) polyclonal antibody was purchased from Cell Signaling (Danvers, MA). Alexa Fluor secondary antibodies and fluorescently labeled phalloidins were purchased from Invitrogen (Carlsbad, CA). Tetramethylrhodamine isothiocyanate (TRITC)-phalloidin was purchased from Sigma (St Louis, MO).

Cell Culture

Mouse embryo fibroblasts (MEFs), MEFs devoid of Src, Yes, and Fyn (SYF) and SYF cells reexpressing cSrc (SYF-cSrc) were obtained from the ATCC (Rockville, MD). Cell lines were cultured in high-glucose Dulbecco modified Eagle medium supplemented with 10% fetal calf serum, 2 mM glutamine, 100 U/ml penicillin, and 100 μg/ml streptomycin.

Study Subjects and Tissue Samples

A total of 280 normal tissues and 124 serous papillary ovarian carcinomas in stage 3 or stage 4 were obtained from the Cooperative Human Tissue Network, Pediatric Division, Children's Hospital, Columbus, OH, and from the West Virginia University Pathology Department. Samples were collected before drug treatment and snap-frozen at −80°C until RNA/DNA extraction was performed. All specimens were diagnosed and classified by pathologists.

Complementary DNA Preparation and Reverse Transcription–Polymerase Chain Reaction

From the studied specimens, total cellular RNA was isolated and purified by hot phenol/chloroform extraction. Purified RNA were precipitated and dissolved in diethyl pyrocarbonate–treated water. Through reverse transcription, using the SuperScript Preamplification System, complementary DNA (cDNA) were generated with oligo-dT primers from 5 μg of total RNA per sample (Reverse Transcription System, Promega, Madison, WI). Exon 9 of the AFAP-110 gene, which contains the SNP for 403C, was amplified by the polymerase chain reaction (PCR). The primer set used for amplification contained the sequence of the 6 intron bases and the 20 exon bases that flank each end of exon 9 (CCGCAGGCTATCTGAACGTGCTCTCC and TCCTACCTCCAATACTGCAACCTCCT). The PCR conditions were 95°C for 3 minutes flowed by 40 cycles at 95°C for 30 seconds, at 58°C for 30 seconds, and at 72°C for 45 seconds and then by 1 cycle at 72°C for 10 minutes.

DNA Sequencing and Genotyping

PCR products were separated on agarose gel and purified using the QIAQuick Gel Extraction Kit (Qiagen, Valencia, CA). The purified fragments were sequenced to identify AFAP-110 mutations using the CEQ 8000 Genetic Analysis System with GenomeLab DTCS-Quick Start Kit (Beckman Coulter, Fullerton, CA) and then using ABI Prism DNA Sequencer with BigDye Terminator Cycle Sequencing Kit (Applied Biosystems, Foster City, CA) to confirm identified mutations. In addition, sequence variants were confirmed in duplicate independent

PCR amplifications and sequencing reactions to ensure that the mutations were not a result of PCR artifact.

Immunohistochemical Methods

Immunohistochemistry (IHC) was performed on 50 serous papillary ovarian carcinomas that were paraffin-embedded and cut into 5-μm-thick sections and mounted on positive charge-coated slides. Tissue sections were dried overnight in a 45°C oven, then deparaffinized, rehydrated, and subjected to heat-induced epitope retrieval for 2 hours in 1 mM citrate buffer (pH 6.00) in an 80°C water bath. Endogenous peroxide activity was blocked with 3% hydrogen peroxide and was followed by treatment with a serum-free protein blocker to block nonspecific binding. After each step of the immunoreaction except the protein blocker, sections were rinsed in Tris-buffered saline with Tween. Tissues were incubated for 2 hours with anti–AFAP-110 antibody (F1, 6 μg/ml) at a dilution of 1:10 or with anti-cSrc (EG107, diluted 1:50) in 10% normal horse serum. Negative controls (i.e., preimmune serum or normal rabbit immunoglobulin G) were incubated in 10% normal horse serum. Sections were incubated with biotinylated secondary link antibody, followed by treatment with streptavidin peroxidase and staining with diaminobenzidine substrate–chromogen solution. Counterstaining was performed with hematoxylin, followed by a water rinse and bluing solution. Tissues were then dehydrated and coverslipped.

Plasmid Constructs

Mutagenesis was performed on human AFAP-110 to generate AFAP-110^{403C}. AFAP-110 and AFAP-110^{403C} were cloned into pEGFP-C3 (Clontech, Mountain View, CA) as previously described [15]. The pGEX-6P-1 vector from Amersham Pharmacia Biotech was used to create fusion proteins expressing the PH2 domain of AFAP as previously described [13]. The pGexX-6P-1 $PH2^{403C}$ construct was created by PCR cloning the $PH2^{403C}$ fragment from the pEGFP vector with *Bam*HI and *Eco*RI ends and subsequent cloning into the pGEX-6P-1 vector. Human AFAP-110 wild-type and $AFAP110^{403C}$ cDNA were PCR-amplified and ligated into pFLAG CMV vector using *Eco*RI and *Xho*I sites to generate Flag-tagged AFAP-110.

Immunofluorescence

Transfection of either GFP AFAP-110 or GFP AFAP-110^{403C} into MEF, SYF, and SYF-cSrc cells for immunofluorescence was carried out using either Lipofectamine PLUS (Invitrogen, Carlsbad, CA) or Nucleofector (Amaxa, Walkersville, MD) according to the manufacturer's specification. Cells were plated on glass coverslips immediately after transfection or allowed to recover for 24 hours after transfection and then plated on glass coverslips coated with 10 μg/ml fibronectin (BD Bioscience, San Jose, CA). Cells were serum starved for 12 hours before fixation or left untreated as indicated in the Results section. Fixation, permeabilization, and staining procedures, including antibody dilutions, were performed as previously described [14]. Confocal images were acquired with a Zeiss LSM 510 microscope with an average slice thickness of 1 μm. Fluorescence channels were sequentially recorded using the multitrack recording module. Fluorescence images were obtained with a Zeiss Axiovert 200M microscope (Thornwood, NY). Images were subsequently analyzed with LSM 510 software, Adobe Photoshop, and Image J (Rasband, WS, ImageJ, US National Institutes of Health, Bethesda, MD; http://rsb.info.nih.gov/ij/, 1997–2007).

Quantification of Podosomes

Actin-rich structures at the ventral surface of cells were identified as podosomes if three podosome markers: AFAP-110, cortactin, and phospho-cSrc colocalized. About 250 to 300 cells from two independent experiments were analyzed to determine the percentage of cells forming podosomes. The number of podosomes/cell was also counted from at least 100 podosome-positive cells, and the distribution of podosomes/cell was plotted. Student's *t* test with Bonferroni adjustment was used to detect the statistical significance.

Western Blot Analysis and cSrc Activation Assay

Cultures or human ovarian tissue were lysed or homogenized in radioimmunoprecipitation assay buffer (50 mM Tris-HCl, pH 7.4, 150 mM NaCl, 2 mM EDTA, 1% NP-40) containing leupeptin, aprotinin, sodium vanadate, EGTA, and phenylmethylsulfonyl fluoride. Protein concentration was determined by the bicinchoninic acid assay (Thermo Fisher Scientific, Rockford, IL), and equal amount of proteins were resolved on SDS-PAGE and transferred to polyvinylidene fluoride. SYF cells were transfected with either Flag-AFAP-110 or Flag-AFAP-110^{403C}, and cSrc cells were transfected using Lipofectamine PLUS (Invitrogen). Forty-eight hours after transfection, cells were stimulated and lysed in radioimmunoprecipitation assay buffer. The levels of phosphorylated Y416 cSrc and total cSrc were assessed in the subsequent Western blot analysis. Antibody dilutions were performed according to previously described protocols [14].

Molecular Modeling

The PH domain of SKAP-hom (PDB ID no. 1U5E), a SKAP55 homolog and a Src-associated adaptor protein, was used as a structural template to create a homology model of the AFAP PH2-WT domain using the homology module of Insight II. Accelrys (San Diego, CA) SKAP-hom was chosen as the best template based on a BLAST server analysis and fold recognition programs such as PHYRE, 123D+, and FUGUE. A sequence alignment was created using the Clustal W server, and manual adjustments were made by integrating secondary structure prediction data for the PH2-WT domain from the PROF server with the known secondary structure 4of SKAP-hom. The model was then minimized with 1000 steps of steepest descent minimization. The structure was equilibrated for 300 ps using explicit water molecules as solvent. Equilibration was completed using the sander command of Amber 8. The model was analyzed to ensure no misfolded regions existed using the Profiles3D program in Insight II. The sander command of Amber 8 (Amber, San Francisco, CA) was then used to create a 700-ps trajectory of the protein domain in explicit water molecules, and a hydrogen bond analysis for $PH2^{403S}$ was completed using the default parameters of the ptraj hbond command in Amber 8. This process was repeated for $PH2^{403C}$.

Lipid Dot-blot

The lipid dot-blot was used to detect interactions between soluble GST proteins and phospholipids immobilized on nitrocellulose. Lipid spotted membranes (PIP strips; Echelon Biosciences, Salt Lake City, UT) were blocked for 1 hour with 0.2% BSA in TBS and incubated overnight with 0.5 mg/ml recombinant GST protein in TBS. Bound GST protein was detected with rabbit anti-GST antibody (Sigma-Aldrich, St Louis, MO).

Preparation of Lipid Vesicles

Large unilamellar lipid vesicles were prepared by the extrusion method using 1-palmitoyl-2-oleoyl-*sn*-glycero-3-phosphocholine (POPC) and

the indicated lipid (Avanti Polar Lipids, Alabaster, AL). Phospholipids were combined by molar ratio (10% indicated lipid–90% POPC or 100% POPC) in chloroform–methanol–water (60:30:4), dried with a stream of N_2, and evacuated to remove traces of solvent. The residue was hydrated with Buffer B (50 mM HEPES, pH 7.2, 80 mM KCl, and 3 mM EGTA) to attain 2 mM lipid sheets when resuspended by vortex. Samples were subjected to 10 cycles of freeze thaw and then 10 passages through two layers of 0.10 μm polycarbonate filters under high pressure N_2. The resulting large unilamellar lipid vesicles were used directly for sedimentation assays.

Sedimentation Assay for PtdIns Lipids

To detect pleckstrin homology domain protein associated with membrane phospholipids, a sedimentation assay was used. Samples containing 1.7 mM vesicle lipid and 0.025 mM recombinant GST fusion protein (PH1) were prepared in 150 μl of binding buffer. Samples were incubated 60 minutes and centrifuged with a Beckman Airfuge (Beckman Coulter, Brea, CA) for 15 minutes at room temperature. From each centrifuged sample, 16% of the supernatant and 100% of the pellet were analyzed by SDS-PAGE. Gels were stained with SPYRO orange (Invitrogen).

Results

AFAP-110 and cSrc Are Overexpressed in Ovarian Cancer

IHC determined that AFAP-110 and cSrc were overexpressed in 30 and 32 of 33 ovarian cancer samples, respectively (Table W1). In 60% of the samples, AFAP-110 was overexpressed focally (Figure 1, *A* and *B*), whereas in 86% of samples, cSrc expression was diffuse (Figure 1, *C* and *D*). AFAP-110 expression in blood vessels is observed in Figure 1*B*.

AFAP-110 and cSrc were not detected in normal ovaries (Figure 2, *A–C*), although blood vessels exhibited AFAP-110 expression (Figure 2*A*). AFAP-110 was always expressed with cSrc in well-differentiated tumors (Figure 2, *D–F*). Further, AFAP-110 and cSrc always colocalized in desmoplastic regions (Figure 2, *G–I*). AFAP-110 is overexpressed in undifferentiated tumor specimens (13 specimens analyzed), but coexpression of AFAP-110 and cSrc was observed in only four of these specimens (Figure 2, *J–L*).

A SNP in AFAP-110

Genetic variation within AFAP-110 was examined. Analysis of AFAP-110 cDNA isolated from the ovarian cancer cell lines OVCAR-3 and 2008 revealed a synonymous SNP (G297A, CCG to CCA) not found in the A2780, MCAS, or SKOV3 lines. A nonsynonymous SNP (C1210G, TCT to TGT) identified in exon 9 resulted in a serine-to-cysteine (S403C) substitution and was also found in the OVCAR-3 and 2008 cell lines.

Ovarian tissues were screened to determine the prevalence of this nonsynonymous SNP, C1210G. C1210G was identified in 19 (20.9%) of 91 tumor samples and in 9 (21.2%) of 41 tumor-adjacent normal tissues (Table W2). In addition, the 33 samples used for IHC were analyzed and revealed the SNP in 9 (27.3%) of 33 samples.

Tissue not associated with cancer was obtained to determine whether the SNP was enriched in ovarian cancer. C1210G was present in

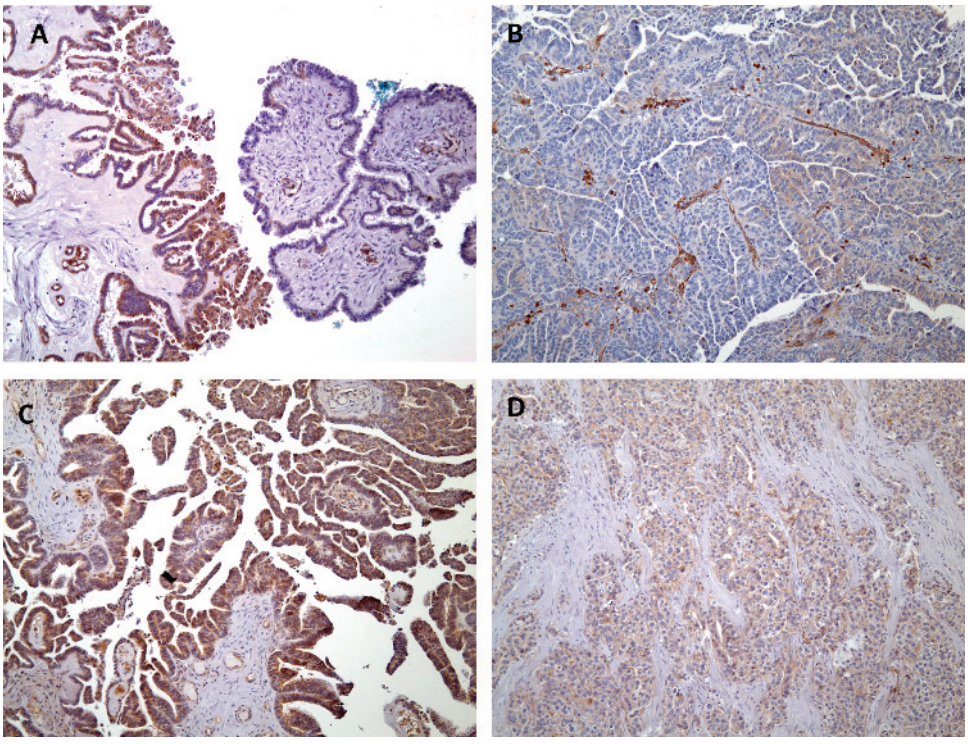

Figure 1. Focal and diffuse expression patterns of AFAP-110 and cSrc. Ovarian cancer tissues were sectioned and IHC performed with anti–AFAP-110 (pAb F1) or anti-cSrc antibody (monoclonal antibody EG107) and the intensity of immunolabeling (brown) qualitatively assessed by a pathologist. Samples that show focal (highly localized) or diffuse immunolabeling that exhibit deep, robust, or weak immunostaining are shown for comparison, and these types of images represent the assessment of tissue immunostaining shown in Table W1. (A) AFAP-110 expressed strongly in focal areas of the tumor. (B) AFAP-110 expressed weakly in focal areas of the tumor. (C) cSrc expressed strongly and diffusely throughout the tumor. (D) cSrc expressed weakly and diffusely throughout the tumor.

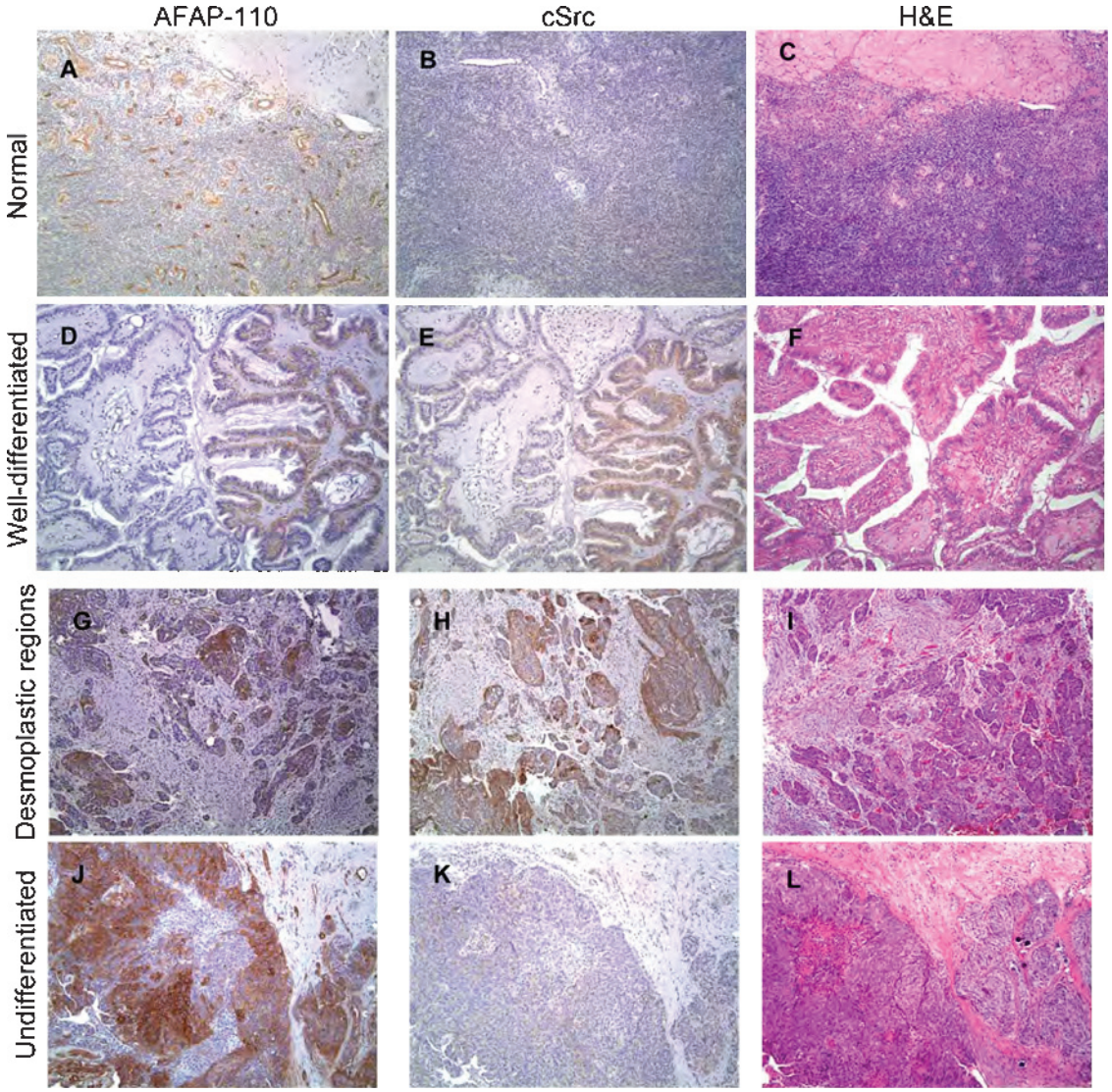

Figure 2. Coexpression of AFAP-110 and cSrc in ovarian tumors. Serial sections of normal human ovary tissues, well-differentiated, and undifferentiated human ovary tissues were immunolabeled for AFAP-110 with pAb F1, cSrc antibody EG107, and hematoxylin and eosin (H&E) staining as described under Materials and Methods: normal ovary/AFAP-110 (A), normal ovary/cSrc (B), normal ovary/H&E (C), well-differentiated tumor/AFAP-110 (D), well-differentiated tumor/cSrc (E), well-differentiated tumor/H&E (F), ovarian tumor/AFAP-110 (G), ovarian tumor/cSrc (H), ovarian tumor/H&E (I), undifferentiated tumor/AFAP-110 (J), undifferentiated tumor/cSrc (K), and undifferentiated tumor/H&E (L). In comparison to normal human ovaries (A–C), AFAP-110 and cSrc protein are overexpressed and colocalized in well-differentiated tumors (D–F), as well as desmoplastic regions of human ovarian tumors (G–I). AFAP-110 is overexpressed in undifferentiated tissue specimens (J–L); however, colocalization with cSrc was variable. All images were captured at a magnification of 100×. As stated in Table W1, 33 ovarian tumors were analyzed. Of these, 20 were differentiated tumors and 13 were undifferentiated. Six normal ovaries were analyzed.

80 (28.6%) of 280 normal tissues (Table W2). Thus, AFAP-110^{403C} was not enriched in ovarian cancer.

We analyzed ovarian tumor tissues and adjacent normal tissue to confirm that cSrc was overexpressed in tissues that have either wild-type AFAP-110 or AFAP-110^{403C}. For comparison, we analyzed the intensity of cSrc expression in SYF cells, which have no Src family kinases [18], and SYF-cSrc cells, which overexpress cSrc. Western blot analysis revealed that cSrc expression in tumors approximated that detected in SYF-cSrc cells (Figure 3*A*). An antibody that detected both forms of AFAP-110 indicated a reduction of AFAP-110 expression in adjacent normal tissues, confirming the overexpression in tumors observed by IHC (Figure 3*B*). Overexpression of cSrc in ovarian tumor samples was also confirmed.

403C Is Located within the PH2 Domain

The serine-to-cysteine (S403C) substitution is located in the second PH domain (PH2) of AFAP-110. PH domains are characterized by seven β-strands that are linked by loop regions. These loop regions differ in length and amino acid composition and therefore confer the differential binding of PH domains to lipids [19–25]. The S403C substitution occurs in a loop region between the fifth and sixth β-strand (Figure 4). In AFAP-110, the hydroxyl *R*-group of Ser^{403} is predicted to interact with water 71% of the time (Figure 4*B*). However, in AFAP-110^{403C}, the sulfhydryl *R*-group of Cys^{403} is not predicted to be an efficient hydrogen binding partner (36%; Figure 4*D*), indicating that the PH^{403C} domain may exhibit differential binding specificity secondary to changes in structural flexibility.

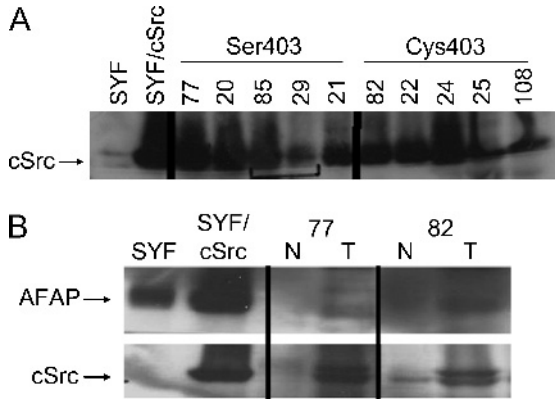

Figure 3. cSrc expression level in ovarian tumors match those levels detected in SYF-cSrc cells. (A) Fifty micrograms of SYF or SYF-cSrc cellular lysates or human ovarian tissue lysates was resolved by 8% SDS-PAGE and transferred to PVDF, and Western blot analysis was performed with anti-cSrc antibodies. Code numbers for deidentified patient samples are shown. Five samples had Ser^{403} encoded on at least one allele, and five samples had Cys^{403} encoded on at least one allele. (B) cSrc and AFAP-110 expression levels are increased in ovarian tumors relative to normal, adjacent tissue. Western blot analysis with antibodies to AFAP-110 or cSrc of two ovarian tumor samples (T) and matching, adjacent control tissues (N) from two patient samples (nos. 77 and 82). Patient no. 77 has the AFAP-110 Ser^{403} wild-type isoform, whereas patient no. 82 has the AFAP-110 Cys^{403} SNP on at least one allele.

PH domains participate in protein-protein interactions. For example, PH domains in pleckstrin and in AFAP-110 (PH1) bind to PKCα [15,26]. Further, the PH1 domain of AFAP-110 binds to AFAP-110, stabilizing the AFAP-110 multimer [13]. To determine differential binding between AFAP-110 and AFAP-110^{403C}, affinity precipitation assays using GST fusion proteins were performed. GST-PH2 was more efficient than GST-$PH2^{403C}$ in pulling down AFAP-110 (Figure 5). CaOV3 cell lysates were used as a negative control because they have AFAP-110 expression levels that are at or below detection limits [14]. These data indicated that the S403C change may reduce the affinity and therefore the ability of the PH2 domain to bind to AFAP-110. Pull-down assays using GST-PH2 did not reveal other binding partners (data not shown).

PH domains are also known to interact with lipids; however, an analysis of the AFAP-110 PH2 domain demonstrated that it does not contain the conserved basic residues that mediate electrostatic interactions with negatively charged phospholipids (Figure 4, *B* and *D*). A lipid dot-blot analysis as well as a lipid vesicle sedimentation assay was used to determine whether the GST-PH2 fusion protein would bind phosphoinositides (Figure W1, *A* and *B*). Unlike the positive control, the PH domain from DAPP1 [27], GST-PH2 did not bind to phosphoinositides.

Effects of AFAP-110^{403C} on Actin Filament Modulation

Affinity precipitation data indicated that the PH2 domain mediates self-association. Earlier work demonstrated that intermolecular interactions that stabilize self-association had an autoinhibitory effect

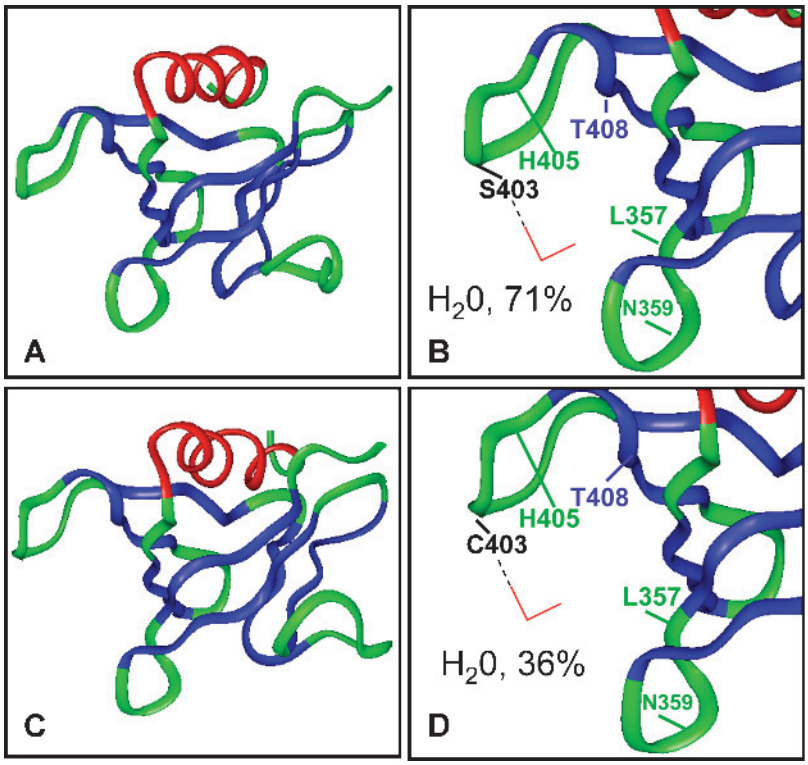

Figure 4. Molecular modeling of the PH2 domain. Homology models for AFAP-110 PH2-WT (A and B) and AFAP-110 $PH2^{403C}$ (C and D) demonstrated that the amino acid change occurs in a loop region between the fifth and sixth β-strand. Performing a hydrogen bond (dashed black lines) analysis for each structure predicted that AFAP-110 PH2-WT binds to water molecules (solid red lines) 71% of the time, potentially forming a rigid binding region. In contrast, AFAP-110 $PH2^{403C}$ was predicted to bind to water only 36% of the time. Labeled amino acids occur at coordinates predicted to interact with phospholipid head groups. Intrastrand loops: green; β-strands: blue; α-helix: red.

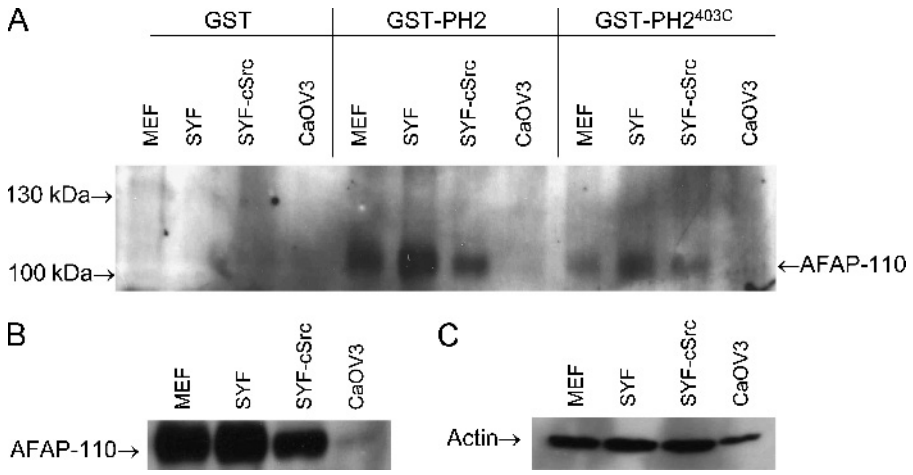

Figure 5. Affinity precipitation of AFAP-110 with GST-PH2 and GST-PH2^{403C}. GST affinity precipitation experiment comparing the differential ability of GST-PH2 and GST-PH2^{403C} to bind AFAP-110 in MEF, SYF, SYF-cSrc, and CaOV3 cell lysates (A). Equal quantities of GST fusion proteins were used to affinity precipitate AFAP-110 from equal amounts of cell lysates. (A) Western blot analysis with pAb F1 indicate that GST-PH2 is more efficient in binding AFAP-110 then GST-PH2^{403C}. CaOV3 cells serve as the negative control in these experiments because this cell line has low to undetectable amount of AFAP-110. Western blots of cell lysates for AFAP-110 (B) and actin loading controls (C) are also shown.

on AFAP-110 [13]. Because GST-PH2^{403C} is less efficient in binding to AFAP-110 than GST-PH2 and destabilization of the AFAP-110 multimer correlated with an acquired ability to activate cSrc, we sought to determine whether AFAP-110^{403C} had the capacity to activate cSrc.

Cotransfection of Flag-tagged AFAP-110 or Flag-tagged AFAP-110^{403C} with cSrc into SYF cells confirmed that AFAP-110^{403C} was able to direct cSrc activation in contrast to wild-type AFAP-110 (Figure 6*A*). The SYF cell lines allowed us to determine the effect of AFAP-110 on cSrc activity in the absence of other Src family members. These data indicated that AFAP-110^{403C} can activate cSrc in cells under conditions of dual overexpression.

To further examine the effect of 403C on the function of AFAP-110, fibroblasts expressing varying levels of cSrc were used. SYF cells do not express cSrc, MEFs express a low level, whereas SYF-cSrc cells express a relatively high level of cSrc (Figure 6*B*). Neither GFP-AFAP-110 nor GFP-AFAP-110^{403C} affected detectable changes in cellular morphology in SYF (data not shown) or in MEF cells (Figure 7*A*). Anti–phospho cSrcY416, which recognizes phosphorylated tyrosine 416 in active cSrc, was used to assess cSrc activity. Active cSrc was undetectable in both SYF and MEF cells. However, in SYF-cSrc cells, GFP-AFAP-110^{403C} directed cSrc activation and the formation of podosomes (Figure 7*B*). Podosome formation was confirmed based on the colocalization of AFAP-110, actin, and cortactin in punctate structures on the ventral surface of the cells [28] (Figure 7*C*). By quantifying the number of cells exhibiting podosomes and the number of podosomes/cell, we determined that podosome formation was strongly associated with expression of AFAP-110^{403C} in SYF-cSrc cells and that cells expressing AFAP-110^{403C} had significantly more podosomes/cell than that of cells expressing only endogenous or overexpressed AFAP-110 (Figure 8).

Discussion

Ovarian cancer results from a combination of inherited and acquired genetic alterations as well as from environmental influences. Detection is limited because of inadequate screening and nonspecific symptoms. Because this leads to a delayed diagnosis, ovarian cancer is the most lethal gynecologic malignancy. This creates interest in identifying biomarkers that stratify patients into high-risk subgroups, as well as potentially guide the development of individualized therapy. The present study demonstrates that AFAP-110^{403C} results in activation of cSrc under conditions of overexpression. Therefore, we hypothesize that the presence and expression levels of AFAP-110^{403C} may have value in predicting risk and treatment strategies for ovarian cancer.

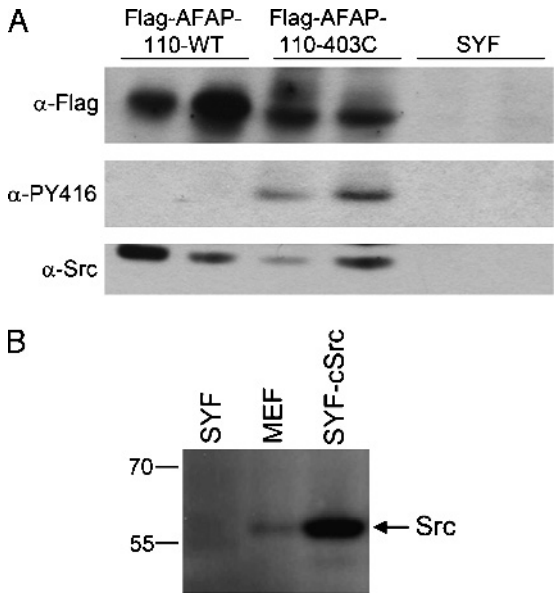

Figure 6. cSrc activity in SYF cells expressing cSrc and AFAP-110^{403C}. (A) Flag-tagged AFAP-110 or AFAP-110^{403C} was transfected into SYF-cSrc cells, and expression levels were detected with anti-Flag antibodies. cSrc expression levels and immunoreactivity with anti-pSrc416 antibodies were determined. (B) Fifty micrograms of MEF, SYF, or SYF-cSrc cellular lysates was resolved by 8% SDS-PAGE and transferred to PVDF, and cSrc was detected with anti-cSrc antibodies.

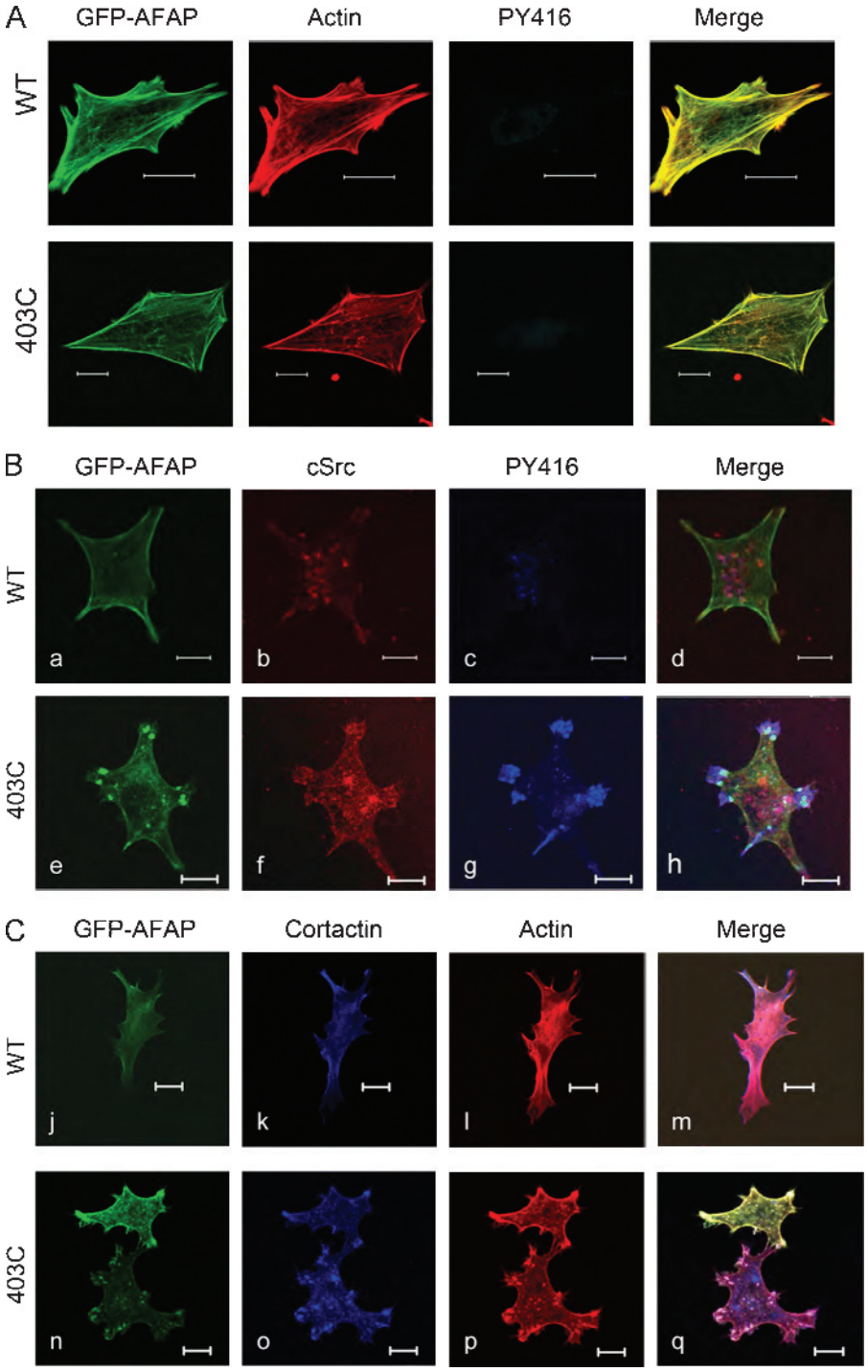

Figure 7. cSrc activation and podosome formation in SYF-cSrc cells expressing AFAP-110^{403C}. (A) MEF cells were transfected with GFP-AFAP-110 or GFP-AFAP-110^{403C} and analyzed for activation of endogenous cSrc or changes in actin filament integrity and podosome formation. Bars, 20 μm. (B) SFY-cSrc cells similarly transiently transfected with GFP-AFAP-110 or GFP-AFAP-110^{403C} and immunolabeled with anti-Src antibody (b and f) and phospho-Src family (Y416) antibody (c and g). Unlike wild-type GFP-AFAP-110, expression of GFP-AFAP-110^{403C} resulted in the formation of punctate structures on the ventral surface of the cells enriched for GFP-AFAP-110^{403C} (e) that exhibited an increase in c-Src phosphorylation at the Y416 position (merged image, h). (C) Punctate structures resulting from the expression of GFP-AFAP-110^{403C} were also enriched for actin and cortactin (merged image, q). In contrast, cells expressing wild-type GFP-AFAP-110 maintained actin filaments and did not exhibit the formation of actin-rich podosomes (j–m). Bars, 10 μm (panels a–d, e–h, n–q) and 20 μm (panels j–m).

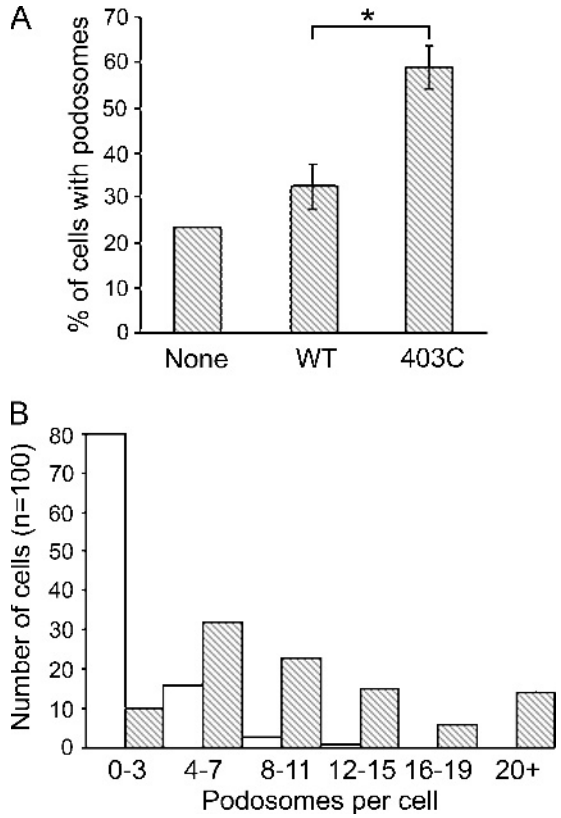

Figure 8. AFAP-110^{403C} directed podosome formation in SYF-cSrc cells. (A) Podosomes were counted in the transfected cells, and the percentage of cells expressing podosomes was quantified (*P = .015, n = 500 cells). (B) The number of podosomes per cell was quantified. The podosome distribution was determined by comparing AFAP-110 to AFAP-110^{403C}. Whereas 80% of the cells transfected with AFAP-110 wild type (empty bars) exhibit between 0 and three podosomes/cell, cells transfected with AFAP-110^{403C} (hatched bars) exhibit a broad distribution with greater than 50% exhibiting more than eight podosomes per cell.

AFAP-110 functions as an actin filament cross-linking protein and an adaptor protein that relays signals from PKCα that activate cSrc [13,15,29–31]. Activated cSrc leads to an increase in cell motility and the production of podosomes, which may be precursors to invadopodia [14,16]. Because podosome formation requires both cSrc activation and dynamic changes in actin filament integrity, AFAP-110 may be uniquely positioned to regulate these two cellular signals. This ability to activate cSrc and contribute to the formation of invasive structures may be relevant for cancer progression [32].

As AFAP-110 is a cSrc activating protein, this report determined whether its expression or its genetic variant AFAP-110^{403C} was associated with ovarian cancer. IHC demonstrated that both AFAP-110 and cSrc were overexpressed in ovarian cancer. In general, cSrc expression was diffuse, whereas AFAP-110 expression was focal. Interestingly, both AFAP-110 and cSrc were always overexpressed together in well-differentiated tumors and in desmoplastic regions of the tumor. Colocalization in desmoplastic areas may represent dynamic interactions between the host and the invasive tumor. As cSrc activation correlates with acquisition of the invasive phenotype [33], we hypothesized that AFAP-110 is positioned to activate cSrc and therefore promote invasion in these discrete areas.

AFAP-110 was scanned for genetic changes in human ovarian cancer cell lines by isolating the cDNA of AFAP-110. A SNP was identified that affected a nonsynonymous coding change at base pair 1210, changing Ser^{403} → Cys^{403}. In addition, 124 ovarian tumors were analyzed and determined to contain the SNP in 22% of the samples. Adjacent, normal ovarian tissue as well as that obtained from women with no known history of malignancy revealed a similar SNP profile. Thus, although expression levels of AFAP-110 were elevated in ovarian cancer, the presence of the SNP was not enriched in tumors. Therefore, this study focused on determining whether high expression levels of AFAP-110 or AFAP-110^{403C} affected differences in cSrc activation or cell morphology.

Serine 403 of AFAP-110 is positioned on the loop between the fifth and sixth β-strands of the PH2 domain. Molecular modeling indicated that the peripherally positioned *R*-hydroxyl group of Ser^{403} forms hydrogen bonding with H_2O 71% of the time, whereas the Cys^{403} forms hydrogen bonding with H_2O less efficiently (36%). Hydrogen bonds may stabilize the loops of the PH domain and increase the rigidity in the binding pocket.

There are as many as 258 different proteins that contain PH domains [34,35]. Of these, only 10% are predicted to facilitate phospholipid binding by forming interactions between positively charged Lys or Arg residues within the PH binding pockets and the negatively charged phospholipids. The PH2 domain of AFAP-110 is unable to bind phospholipid.

PH domains also bind to proteins. Affinity precipitation revealed that similar to the PH1 domain, the PH2 domain also bound AFAP-110. Thus, it is predicted that the PH2 domain may foster either intramolecular or intermolecular interactions, promoting multimerization or stabilization of the multimer. However, GST-PH2^{403C} bound less efficiently to AFAP-110. Loss of AFAP-110 multimer stability correlated with a gain-of-function, including an ability to colocalize and activate cSrc [13,14,16]. Thus, we sought to determine whether AFAP-110^{403C} activates cSrc.

Expression of AFAP-110 or AFAP-110^{403C} in MEF cells, which contain detectable levels of cSrc, estimated around 20,000 molecules per cell (D.C. Flynn, unpublished observations), did not result in cSrc activation or morphologic changes that are associated with cSrc activation. Ectopically expressed AFAP-110 or AFAP-110^{403C} in SYF-cSrc cells, which overexpress cSrc at levels that are higher than MEFs, was used to determine whether AFAP-110^{403C} has a differential capacity to activate cSrc. Compared with AFAP-110, AFAP-110^{403C} was a more efficient activator of cSrc and was more efficient in inducing the formation of podosomes. Thus, these data indicate that in cells overexpressing cSrc, AFAP-110^{403C} more efficiently activates cSrc compared with wild-type AFAP-110. Previous evidence suggested that, in chicken embryo fibroblasts transformed by the Rous sarcoma virus, only 5% of AFAP-110 is complexed with v-Src [31]. Because only a subset of AFAP-110 and Src interact, it is possible that, in MEF cells, only 5% or less of the cSrc population that is expressed would be engaged with AFAP-110^{403C} and that this stoichiometry of binding could be below detection. Further, if 5% of cSrc were activated in MEF cells, activation may be insufficient to direct morphologic changes characteristic of Src-transformed cells. Thus, under conditions where both cSrc and AFAP-110^{403C} expression is low, as in normal tissues, cSrc activation is unlikely to occur or affect cellular changes even in those cells that inherit AFAP^{403C}. Under conditions of dual overexpression of AFAP-110^{403C} and cSrc, AFAP-110^{403C} may independently activate cSrc and promote tumor progression. Because AFAP-110 and cSrc are overexpressed in the same tumors, AFAP-110 may enhance cSrc activation by receiving input signals that enable cSrc activation, or alternatively, AFAP-110^{403C} may result in a

reduced capacity to self-associate resulting in the independent activation of cSrc. Although not enriched in ovarian cancer tumors, the 403C variant may lead to a more aggressive and metastatic disease through its promotion of cSrc activation in those tumors in which it is found. Future studies using ovarian cancer cell lines and additional patient samples should address this issue. These data also indicate a mechanism by which an inherited genetic variation could influence ovarian cancer progression and could be used to predict the response to targeted therapy.

References

[1] Naora H and Montell DJ (2005). Ovarian cancer metastasis: integrating insights from disparate model organisms. *Nat Rev Cancer* **5**, 355–366.

[2] Jemal A, Siegel R, Ward E, Murray T, Xu J, and Thun MJ (2007). Cancer statistics, 2007. *CA Cancer J Clin* **57**, 43–66.

[3] Pal T, Permuth-Wey J, Betts JA, Krischer JP, Fiorica J, Arango H, LaPolla J, Hoffman M, Martino MA, Wakeley K, et al. (2005). *BRCA1* and *BRCA2* mutations account for a large proportion of ovarian carcinoma cases. *Cancer* **104**, 2807–2816.

[4] Risch HA, McLaughlin JR, Cole DE, Rosen B, Bradley L, Fan I, Tang J, Li S, Zhang S, Shaw PA, et al. (2006). Population *BRCA1* and *BRCA2* mutation frequencies and cancer penetrances: a kin-cohort study in Ontario, Canada. *J Natl Cancer Inst* **98**, 1694–1706.

[5] Goldstein DB and Cavalleri GL (2005). Genomics: understanding human diversity. *Nature* **437**, 1241–1242.

[6] Reyes-Gibby CC, Wu X, Spitz M, Kurzrock R, Fisch M, Bruera E, and Shete S (2008). Molecular epidemiology, cancer-related symptoms, and cytokines pathway. *Lancet Oncol* **9**, 777–785.

[7] Wiener JR, Windham TC, Estrella VC, Parikh NU, Thall PF, Deavers MT, Bast RC, Mills GB, and Gallick GE (2003). Activated SRC protein tyrosine kinase is overexpressed in late-stage human ovarian cancers. *Gynecol Oncol* **88**, 73–79.

[8] Frame MC (2004). Newest findings on the oldest oncogene; how activated src does it. *J Cell Sci* **117**, 989–998.

[9] Yeatman TJ (2004). A renaissance for SRC. *Nat Rev Cancer* **4**, 470–480.

[10] Chen T, Pengetnze Y, and Taylor CC (2005). Src inhibition enhances paclitaxel cytotoxicity in ovarian cancer cells by caspase-9–independent activation of caspase-3. *Mol Cancer Ther* **4**, 217–224.

[11] George JA, Chen T, and Taylor CC (2005). SRC tyrosine kinase and multidrug resistance protein-1 inhibitions act independently but cooperatively to restore paclitaxel sensitivity to paclitaxel-resistant ovarian cancer cells. *Cancer Res* **65**, 10381–10388.

[12] Baisden JM, Gatesman AS, Cherezova L, Jiang BH, and Flynn DC (2001). The intrinsic ability of AFAP-110 to alter actin filament integrity is linked with its ability to also activate cellular tyrosine kinases. *Oncogene* **20**, 6607–6616.

[13] Qian Y, Gatesman AS, Baisden JM, Zot HG, Cherezova L, Qazi I, Mazloum N, Lee MY, Guappone-Koay A, and Flynn DC (2004). Analysis of the role of the leucine zipper motif in regulating the ability of AFAP-110 to alter actin filament integrity. *J Cell Biochem* **91**, 602–620.

[14] Gatesman A, Walker VG, Baisden JM, Weed SA, and Flynn DC (2004). Protein kinase Cα activates c-Src and induces podosome formation via AFAP-110. *Mol Cell Biol* **24**, 7578–7597.

[15] Qian Y, Baisden JM, Cherezova L, Summy JM, Guappone-Koay A, Shi X, Mast T, Pustula J, Zot HG, Mazloum N, et al. (2002). PC phosphorylation increases the ability of AFAP-110 to cross-link actin filaments. *Mol Biol Cell* **13**, 2311–2322.

[16] Walker VG, Ammer A, Cao Z, Clump AC, Jiang BH, Kelley LC, Weed SA, Zot H, and Flynn DC (2007). PI3K activation is required for PMA-directed activation of cSrc by AFAP-110. *Am J Physiol Cell Physiol* **293**, C119–C132.

[17] Qian Y, Guappone AC, Baisden JM, Hill MW, Summy JM, and Flynn DC (1999). Monoclonal antibodies directed against AFAP-110 recognize species-specific and conserved epitopes. *Hybridoma* **18**, 167–175.

[18] Klinghoffer RA, Sachsenmaier C, Cooper JA, and Soriano P (1999). Src family kinases are required for integrin but not PDGFR signal transduction. *EMBO J* **18**, 2459–2471.

[19] Haslam RJ, Koide HB, and Hemmings BA (1993). Pleckstrin domain homology. *Nature* **363**, 309–310.

[20] Mayer BJ, Ren R, Clark KL, and Baltimore D (1993). A putative modular domain present in diverse signaling proteins. *Cell* **73**, 629–630.

[21] Musacchio A, Gibson T, Rice P, Thompson J, and Saraste M (1993). The PH domain: a common piece in the structural patchwork of signalling proteins. *Trends Biochem Sci* **18**, 343–348.

[22] Yoon HS, Hajduk PJ, Petros AM, Olejniczak ET, Meadows RP, and Fesik SW (1994). Solution structure of a pleckstrin-homology domain. *Nature* **369**, 672–675.

[23] Macias MJ, Musacchio A, Ponstingl H, Nilges M, Saraste M, and Oschkinat H (1994). Structure of the pleckstrin homology domain from beta-spectrin. *Nature* **369**, 675–677.

[24] Lemmon MA, Ferguson KM, O'Brien R, Sigler PB, and Schlessinger J (1995). Specific and high-affinity binding of inositol phosphates to an isolated pleckstrin homology domain. *Proc Natl Acad Sci USA* **92**, 10472–10476.

[25] Hyvonen M, Macias MJ, Nilges M, Oschkinat H, Saraste M, and Wilmanns M (1995). Structure of the binding site for inositol phosphates in a PH domain. *EMBO J* **14**, 4676–4685.

[26] Abrams CS, Zhao W, Belmonte E, and Brass LF (1995). Protein kinase C regulates pleckstrin by phosphorylation of sites adjacent to the N-terminal pleckstrin homology domain. *J Biol Chem* **270**, 23317–23321.

[27] Dowler S, Currie RA, Downes CP, and Alessi DR (1999). DAPP1: a dual adaptor for phosphotyrosine and 3-phosphoinositides. *Biochem J* **342** (pt 1), 7–12.

[28] Linder S and Aepfelbacher M (2003). Podosomes: adhesion hot-spots of invasive cells. *Trends Cell Biol* **13**, 376–385.

[29] Dorfleutner A, Stehlik C, Zhang J, Gallick GE, and Flynn DC (2007). AFAP-110 is required for actin stress fiber formation and cell adhesion in MDA-MB-231 breast cancer cells. *J Cell Physiol* **213**, 740–749.

[30] Chen WT, Chen JM, Parsons SJ, and Parsons JT (1985). Local degradation of fibronectin at sites of expression of the transforming gene product pp60src. *Nature* **316**, 156–158.

[31] Kanner SB, Reynolds AB, and Parsons JT (1991). Tyrosine phosphorylation of a 120-kilodalton pp60src substrate upon epidermal growth factor and platelet-derived growth factor receptor stimulation and in polyomavirus middle-T-antigen–transformed cells. *Mol Cell Biol* **11**, 713–720.

[32] Flynn DC, Cho YJ, Vincent D, and Cunnick JM (2008). Podosomes and invadopodia: related structures with common protein components that may promote breast cancer cellular invasion. *Breast Cancer (Auckl)* **2**, 17–29.

[33] Summy JM and Gallick GE (2006). Treatment for advanced tumors: SRC reclaims center stage. *Clin Cancer Res* **12**, 1398–1401.

[34] Lemmon MA, Ferguson KM, and Abrams CS (2002). Pleckstrin homology domains and the cytoskeleton. *FEBS Lett* **513**, 71–76.

[35] McPherson JD, Marra M, Hillier L, Waterston RH, Chinwalla A, Wallis J, Sekhon M, Wylie K, Mardis ER, Wilson RK, et al. (2001). A physical map of the human genome. *Nature* **409**, 934–941.

[36] Dowler S, Currie RA, Downes CP, and Alessi DR (1999). DAPP1: a dual adaptor for phosphotyrosine and 3-phosphoinositides. *Biochem J* **15**, 7–12.

Supplemental Information

Supplemental information is available at www.transonc.com.

Table W1. Summary of IHC Intensity and Pattern of cSrc and AFAP-110 Expression in 33 Ovarian Tumor Samples.

Tumor Sample	F/D (AFAP)	S/W (AFAP)	F/D (Src)	S/W (Src)
1	0	0	D	S
2	F	S	D	W
3	F	W	D	W
4	0	0	D	S
5	F	W	D	W
6	F	W	D	S
7	F	W	D	W
8	F	S	D	S
9	D	S	D	S
10	F	S	D	W
11	D	W	D	W
12	D	S	F	S
13	F	S	D	S
14	F	S	0	0
15	F	W	D	W
16	F	S	D	W
17	D	S	F	W
18	F	W	D	S
19	0	0	F	W
20	F	W	D	W
21	D	S	D	W
22	D	S	D	W
23	F	S	D	S
24	D	S	D	W
25	D	S	F	S
26	D	S	D	W
27	F	S	D	W
28	D	S	F	W
29	D	S	D	S
30	F	S	D	W
31	F	W	D	W
32	F	S	D	W
33	D	S	D	W
Negative		3		1
Positive		30	91%	32
D/S		11		9
D/W		1		18
F/S		10		2
F/W		8		3
Diffuse		12	40%	27
Focal		18	60%	5

D, diffuse immunostaining; *F*, focal immunostaining; *S*, strong intensity; *W*, weak intensity.

Table W2. Presence of C1209G Nonsynonymous SNP in Tissue Samples.

Sample	CC (Wild Type)	CG SNP (One Allele)	GG SNP (Both Alleles)	Total SNP (One or Two Alleles)
Tumor (GoG)	72/91 (79.1%)	18/91 (19.8%)	1/91 (1.1%)	19/91 (20.9%)
Tumor (WVU)	24/33 (72.8%)	7/33 (21.2%)	2/33 (6.1%)	9/33 (27.3%)
Tumor (total)	97/124 (78.2%)	24/124 (19.3%)	3/124 (2.4%)	27/124 (21.7%)
Normal tissue	200/280 (71.4%)	73/280 (26.1%)	7/280 (2.5%)	80/280 (28.6%)

Exon 9 was amplified from 124 ovarian cancer tissue samples and 280 normal tissues. Sequence analysis was performed, and the presence of the wild-type sequence (C on both alleles — CC) or the SNP (G on one allele — CG) or on both alleles (GG) was calculated. In tumor-adjacent normal ovarian tissues, the nonsynonymous SNP was identified in 9 (21.2%) of 41 samples obtained from GoG. *WVU* indicates West Virginia University.

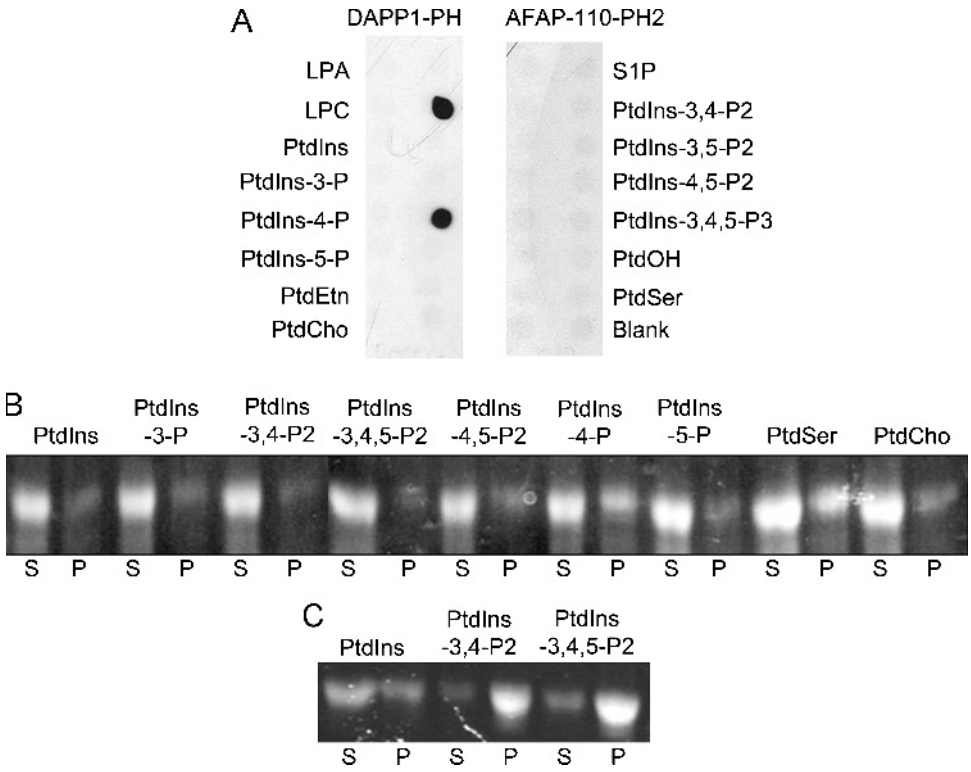

Figure W1. The PH2 domain does not bind to phospholipids. (A) Lipid dot-blot analysis was used to examine the ability of the GST-AFAP-PH2 domain to bind immobilized phospholipids. GST-DAPP1-PH was used as a positive control and bound both PtdIns-3,4-P_2 and PtdIns-3,4,5-P_3 consistent with published data [36]. The GST-AFAP-110-PH2 did not bind any immobilized phosphoinositides tested. (B and C) A lipid vesicle sedimentation assay was performed with GST-PH2 (B) or the positive control GST-DAPP1-PH (C). After SDS-PAGE of the supernatants (S) and the pellets (P), the gels were stained with SYPRO orange. Data are consistent with the lipid dot-blot analysis.